

Large-Eddy Simulation of Sea Spray Impacts on Fluxes in the High-Wind Boundary Layer

 David H. Richter¹  and Charlotte E. Wainwright¹ 
¹Department of Civil and Environmental Engineering and Earth Sciences, University of Notre Dame, Notre Dame, IN, USA

Key Points:

- When sea spray is injected at a realistic rate it does not affect the drag coefficient, C_D , up to 48 m s^{-1}
- High spray production quickly saturates the surface layer, which limits the impact of spray on fluxes and air-sea flux coefficients
- Very little change in the thermodynamic flux coefficients are at wind speeds beyond 36 m s^{-1} if the surface layer saturates

Correspondence to:

 D. H. Richter,
David.Richter.26@nd.edu

Citation:

 Richter, D. H., & Wainwright, C. E. (2023). Large-eddy simulation of sea spray impacts on fluxes in the high-wind boundary layer. *Geophysical Research Letters*, *50*, e2022GL101862. <https://doi.org/10.1029/2022GL101862>

 Received 25 OCT 2022
Accepted 17 JAN 2023

Abstract The exchange of enthalpy and momentum at the air-sea interface is an important process in tropical cyclone (TC) development and intensification, and the effects of sea spray have long been uncertain, particularly at high wind speeds. Here we use a coupled large-eddy simulation and Lagrangian cloud model to run high-resolution simulations of an idealized, spray-laden TC boundary layer. Simulations are performed with and without spray generation, using a realistic sea spray generation function over wind speeds relevant to TCs. We show that C_D is not affected by spray droplets at 10-m wind speeds up to 48 m s^{-1} . C_E and C_H are modified during an initial transient adjustment stage, but quickly relax back to their unladen values due to surface layer saturation. This relaxation occurs faster for higher winds, because the increased spray concentration more rapidly saturates the surface layer.

Plain Language Summary A tropical cyclone ultimately gets its energy from the ocean, and understanding how this energy is transferred from the ocean to the air is important for accurate prediction. In the extreme winds inside of a hurricane, however, the ocean surface is torn into a huge number of sea spray droplets, and for decades researchers have speculated as to how these suspended droplets change the way that heat, moisture, and momentum are delivered to the atmosphere. Since making measurements in these conditions is so difficult, we use realistic, high-resolution simulations to mimic conditions with and without spray to better understand its role. In the highest winds, we find that spray limits its own impact on air-sea transfer by quickly increasing the humidity near the ocean surface.

1. Introduction

Although there have been considerable improvements in forecasting the track of tropical cyclones (TCs) over the past several decades, intensity forecasts remain challenging and improvements have lagged behind (Rogers et al., 2006). One challenge is that the understanding of air-sea exchange in high-wind regimes remains limited due to the logistical difficulty of taking measurements in these conditions. Further complications arise from a lack of knowledge on how the presence of sea spray affects the air-sea fluxes, and how this varies with wind speed (Veron, 2015). Improving parameterizations of air-sea fluxes in numerical models is of particular importance for reducing uncertainty in intensity forecasts (Sroka & Emanuel, 2021).

Key parameters in air-sea exchange are the surface drag coefficient (C_D) and surface enthalpy flux coefficient (C_K), which are known to factor into the maximum storm potential energy and the maximum tangential wind speed (Emanuel, 1995). In numerical weather prediction (NWP) models C_D and C_K (or the individual heat and moisture coefficients, C_H and C_E , often assumed to be equal to C_K) are typically parameterized as functions of the 10-m wind speed (U_{10}). At high winds beyond roughly 30 m s^{-1} , however, the behavior of these flux coefficients are highly uncertain (Richter et al., 2016), and almost certainly not solely a function of wind speed. One factor in particular that is central to our understanding of the transfer of heat and momentum at high wind speeds is the presence of spray droplets. Spray mediation of air-sea fluxes has been the subject of many previous investigations, including theoretical, observational, and numerical modeling approaches, and a comprehensive review on the subject can be found in Veron (2015) or Sroka and Emanuel (2021). Although many numerical modeling studies have investigated the impact of spray on air-sea fluxes, most of these studies have relied on bulk estimates in which the net effect of spray is parameterized rather than handled explicitly.

Here we investigate the impact of sea spray on the transfer coefficients for momentum, heat, and moisture, by performing simulations using a large-eddy simulation (LES) code coupled with a Lagrangian microphysical model. Paired simulations are performed with and without the presence of spray, across a range of wind speeds up

© 2023. The Authors.

 This is an open access article under the terms of the [Creative Commons Attribution License](https://creativecommons.org/licenses/by/4.0/), which permits use, distribution and reproduction in any medium, provided the original work is properly cited.

to $U_{10} = 48 \text{ m s}^{-1}$. Section 2 provides details about the model and the simulation setup used in our experiments. Results are presented in Section 3, and discussion and conclusions are given in Section 4.

2. Modeling Approach

2.1. Numerical Model and Setup

The model used here is the NTLP (National Center for Atmospheric Research Turbulence with Lagrangian Particles) model, which couples LES with Lagrangian droplets in a so-called Lagrangian cloud model (LCM) framework. The underlying LES code is based on the NCAR LES code (Moeng, 1984; Sullivan et al., 1994) and employs the Deardorff (1980) subgrid model. This LES-LCM numerical framework has previously been used to examine cloud microphysics (MacMillan et al., 2022; Richter et al., 2021), and as well as the coupled effects of sea spray on air-sea exchange of heat and moisture (Peng & Richter, 2017, 2019, 2020). The LES-LCM code uses the “superdroplet” concept of Shima et al. (2009), in which a single numerical particle represents a cluster of droplets with the same location, velocity, temperature, composition, and mass. As detailed in Richter et al. (2021), the superdroplets are fully coupled to the background flow, and the Lagrangian equations for mass, momentum, and energy conservation are solved according to full Köhler microphysics for each superdroplet at every timestep based on the turbulent air properties experienced locally by each droplet.

For this study the code has been modified to better mimic conditions in the hurricane boundary layer by implementing the method of Bryan et al. (2017), which alters the horizontal velocity equations to account for advective and centrifugal forces that occur on scales larger than the domain size resulting from storm-scale dynamics. What results is a high-resolution, horizontally periodic “patch” of the hurricane boundary layer where the mean eyewall updraft is unimportant (the instantaneous vertical velocities in the LES are fully resolved, and the turbulence characteristics of a similar setup can be found in Bryan et al. (2017)). The method is based on three input parameters: radial distance from storm center (R), a reference gradient wind speed (V), and the radial decay rate of wind speed ($\partial V/\partial R$), and has been shown to produce realistic turbulent features (Bryan et al., 2017; Chen et al., 2021). Here we choose $R = 40 \text{ km}$ and $\partial V/\partial R = -1.2 \times 10^{-3}$ following the setup of Bryan et al. (2017) which assumes a power-law decay of V with radius (Mallen et al., 2005).

We have also implemented the Andreas (1998) sea spray generation function (SSGF) into the LES-LCM. This SSGF is based on a modified version of that in Smith et al. (1993), and the formulation covers droplets of size $2 \leq r \leq 500 \text{ }\mu\text{m}$, where r is the droplet radius at formation. The droplet number flux is based on U_{10} . An example figure showing how the droplet number and volume concentration vary with U_{10} is seen in Figure 1. The spray composition can be adjusted, and here we assume typical seawater conditions with a salinity of 34 g kg^{-1} . Spray particles are introduced at random locations in the horizontal x and y directions and at a random height below 8 m (to mimic a significant wave height of 8 m). The initial spray horizontal velocity is zero, so that the acceleration of the droplets must come at the expense of the air momentum (a frequently assumed mechanism for spray-mediated momentum fluxes). The vertical ejection velocity has a random value between 0 and 4 m s^{-1} , chosen based on rough estimates from a range of laboratory measurements (see e.g., the summary in Lewis and Schwartz (2004)). We note that many studies have proposed updated SSGFs since Andreas (1998), particularly those which recognize the potential underestimation of large droplet production (Fairall et al., 2009; Ortiz-Suslow et al., 2016; Troitskaya et al., 2018). We use the Andreas (1998) SSGF primarily because it is well-known and easy to implement, while it is still very uncertain how laboratory measurements of large droplets near the wave surface should be extrapolated to the real hurricane boundary layer. This is not to claim that these large droplets are not present or would not necessarily have a strong impact on air-sea fluxes; however their availability at heights where droplets are initialized in the current LES framework remains uncertain. As we argue below, we do not anticipate the primary conclusions of this study to change if different SSGF functions are utilized, even if some of the quantitative details are altered.

We run several pairs of simulations across a range of reference wind speeds. At each wind speed, we perform one simulation in which spray is not included (hereafter “unladen” cases). All of the simulations use the same domain of 128^3 grid points, with 2 m horizontal grid spacing and uniform 1 m vertical grid spacing, and which are periodic in the horizontal directions. A dynamic timestep is used which is adjusted based on the Courant-Friedrichs-Lewy (CFL) condition, and each simulation is run for 2 hr . The second simulation in each pair is first run for 30 min with no spray injection to allow the turbulence to spin up, and after 30 min , spray is injected based on

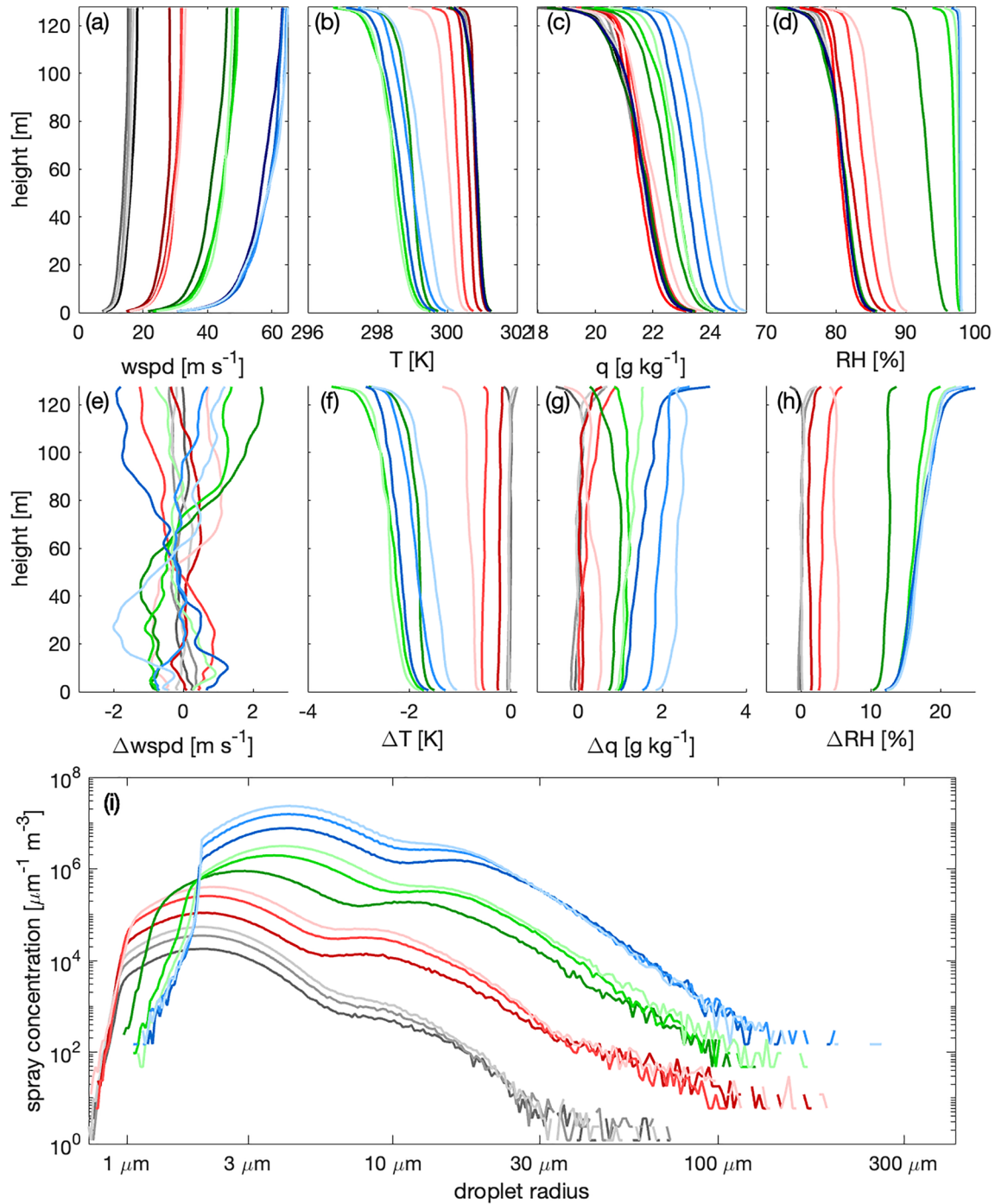


Figure 1. Top row: domain-averaged profiles of wind speed (a), temperature (b), water vapor mixing ratio (c), and relative humidity (d), at 30 min intervals throughout each particle-laden simulation (30, 60, 90, and 120 min). Different colors represent the different wind speeds (L20: gray, L40: red, L60: green, L80: blue), with the darkest color showing the earliest time of 30 min and the color becoming lighter over time (e.g., dark blue is case L80 at 30 min, lightest blue is L80 at 120 min). The middle row shows the difference in profiles between the unladen and particle-laden simulations at 60, 90, and 120 min. Colors and line styles are the same throughout. The lower panel (i) shows the domain-wide sea spray size distribution at the same times.

the Andreas (1998) SSGF. Spray injection continues at the rate prescribed by the SSGF for the rest of the 2 hr simulation.

The lower boundary conditions employ roughness lengths which are set to achieve realistic values of the unladen C_D , C_H , and C_E seen below. To achieve steady-state conditions within the simulation, fluxes of heat, moisture, and

momentum at the top boundary are set to equal the surface interfacial fluxes. The initial temperature and moisture profile used in the simulations is generated based on aggregated dropsonde data (see e.g., the TC-DROPS database, Nguyen et al. (2019)). We selected all dropsonde profiles released at a radius of between 2 and 6 times the radius of maximum winds (RMW), to mimic the numerical setup of a hurricane patch outside the RMW from the method of Bryan et al. (2017). The RMW data used to filter the dropsondes is taken from the extended best track database (EBTRK; Demuth et al., 2006).

2.2. Surface Exchange Coefficients

The traditional method of parameterizing the surface fluxes in NWP models is through the use of transfer coefficients C_D , C_E , and C_H , which are defined by the following expressions:

$$\tau_0 = \rho_a C_D U_{10}^2, \quad (1)$$

$$H_{S0} = \rho_a c_p C_H U_{10} (T_{sfc} - T_{10}), \quad (2)$$

$$H_{L0} = \rho_a L_v C_E U_{10} (q_{sfc} - q_{10}). \quad (3)$$

Here, τ_0 , H_{S0} , and H_{L0} are the total fluxes of momentum ($\tau(z)$), sensible heat ($H_S(z)$), and latent heat ($H_L(z)$), where the “0” subscript refers to evaluating these fluxes at $z = 0$. The bulk flux relationships are typically defined with the 10-m reference wind speed (U_{10}), temperature (T_{10}), and water vapor mixing ratio (q_{10}), and T_{sfc} and q_{sfc} are the sea surface temperature (SST) and surface water vapor mixing ratio q_{sfc} (assuming saturation at the water surface), and surface currents are typically neglected. ρ_a and c_p are the density and specific heat of air, and L_v is the latent heat of vapourization.

In this study, our goal is to resolve turbulence in the hurricane boundary layer, along with its full coupling with a realistic treatment of sea spray, in such a way as to directly compute and compare the flux coefficients with and without the presence of spray droplets. By making the common assumption that the fluxes can be broken down into their turbulent (“turb”) and spray-mediated (“sp”) components (Andreas et al., 2015; Fairall et al., 1994) and rearranging, the flux coefficients can be calculated via

$$C_D = \frac{\tau_{0,turb} + \tau_{0,sp}}{\rho_a U_{10}^2}, \quad (4)$$

$$C_H = \frac{H_{S0,turb} + H_{S0,sp}}{\rho_a c_p U_{10} (T_{sfc} - T_{10})}, \quad (5)$$

$$C_E = \frac{H_{L0,int} + H_{L0,sp}}{\rho_a L_v U_{10} (q_{sfc} - q_{10})}, \quad (6)$$

As detailed in the idealized study of Peng and Richter (2019), so-called bulk spray models, which aim to parameterize the spray-mediated components of the fluxes, must make certain assumptions regarding the various potential couplings. The simplest approximation is to assume that the surface spray components $\tau_{0,sp}$, $H_{S0,sp}$, and $H_{L0,sp}$ are simply additive, in that the surface turbulent (also referred to as “interfacial”) fluxes and the 10-m reference conditions are unchanged with the addition of spray. In reality, however, the heat, moisture, and momentum carried by the spray can (and does) change both the 10-m reference conditions, as well as the interfacial fluxes carried by the turbulent motions in the air. Some bulk spray models, such as those by Bao et al. (2011) and Barr et al. (2023), attempt to incorporate these various couplings, but in the present case these couplings are naturally included.

We perform a straightforward series of LES-LCM simulations, where four wind speeds are run with and without spray. They are driven by reference wind speeds of $V = [20, 40, 60, 80]$ m s⁻¹, which correspond to 10-m wind speeds of $U_{10} = [12, 24, 36, 48]$ m s⁻¹. Throughout, a prefix “U” refers to the unladen simulation at a particular wind speed, while “L” refers to the spray-laden simulation (e.g., U20 is the unladen, $V = 20$ m s⁻¹ case). In each fully coupled simulation we directly calculate the turbulent and spray-mediated components of momentum, sensible, and latent heat fluxes, as well as their impact on the 10-m reference conditions, in order to observe the impact of spray on the effective flux coefficients in Equations 4–6.

3. Results

Domain-averaged profiles from each of the laden simulations are shown at several time steps in the upper row of Figure 1. As time evolves (dark to light shading depicts 30-min intervals), the effects of spray at each wind speed (denoted by color) are observed. The middle row of Figure 1 shows the difference in the wind, temperature, moisture, and relative humidity (RH) profiles between the laden and unladen cases at 60, 90, and 120 min (again denoted with line transparency).

No clear systemic difference is visible in the wind profiles between the laden and unladen cases (Figures 1a and 1e; note that the wind profiles are still slightly evolving at the time of injection). However, the spray injection does alter the temperature, moisture and RH profiles significantly. The presence of sea spray reduces the temperature (Figures 1b and 1f) and increases the mixing ratio (Figures 1c and 1g), thus increasing the RH (Figures 1d and 1h). This is consistent with the conceptual picture of Fairall et al. (1994) and the one-dimensional modeling of Rastigejev and Suslov (2019). The differences in the thermodynamic profiles due to the presence of spray cases generally increases over time as spray injection continues (Figures 1f–1h) at all wind speeds, with the exception of the temperature profile for case L80, where the largest temperature difference occurs at 60 min and decreases thereafter (Figures 1b and 1f). In general larger differences in the thermodynamic profiles are seen at higher wind speeds, owing to the larger production of spray.

Figure 1i shows the sea spray size distribution at 60, 90, and 120 min into each simulation. The distributions shown in Figure 1i are number concentrations calculated across the entire domain, despite the fact that the size distributions change rapidly with height, particularly for the large droplets. We can see from Figure 1i that the particle concentration increases with increasing wind speed, as expected, with the exception of large ($r \gtrsim 30 \mu\text{m}$) droplets. For a given wind speed (and thus a given SSGF strength), the large droplets quickly establish an equilibrium, in that their large gravitational settling rapidly approaches their production rate, holding their number constant. It is these “re-entrant” droplets which are known to carry most of the spray-mediated heat and moisture fluxes (Andreas & Emanuel, 2001), precisely because they are rapidly refreshed as time evolves. As the wind speed increases, the likelihood of producing large droplets increases according to the formulation of the SSGF, and therefore more are seen in Figure 1i as the wind speed increases. The minimum particle size introduced by the SSGF is the same in each simulation, and differences seen in lowest particle radius are due to particle interactions with the flow, with lower minimum spray radii seen for lower RH values.

3.1. Impact of Sea Spray on Drag Coefficient (C_D)

We first investigate the impact of sea spray on the bulk drag coefficient C_D . As is evident from Figure 1e, the presence of sea spray does not cause a systematic change in the wind profile even though the spray droplets are fully coupled in momentum. Figures 2a and 2b further show that both τ and U_{10} remain independently unchanged with time for all wind speeds and spray concentrations, leading to C_D values which fluctuate within only a couple of percent different than the unladen C_D value (which itself is dictated by the LES wall model roughness at the lower surface)—see Figures 2c and 2d. It might be expected that at the highest wind speeds, since so many spray droplets are being injected, the droplets' momentum could accelerate the wind speed (or otherwise reduce the drag coefficient via acting as a source of density stratification) but we do not see any evidence for this, in contrast with a number of models (Barenblatt et al., 2005). As such, it follows that the drag coefficient will not be altered by the presence of spray droplets, and this is what we see in Figure 2c.

3.2. Impact of Sea Spray on Heat and Moisture Transfer Coefficients (C_H and C_E)

We next examine the impact of sea spray on C_H and C_E . The total (i.e., interfacial plus spray) surface sensible and latent heat fluxes H_{S0} and H_{L0} are shown in Figures 2e and 2i, and highlight the impact that spray has on fluxes through the surface layer. While more details can be found elsewhere (Andreas & Emanuel, 2001; Fairall et al., 1994), recall that in the simplest terms a droplet in a uniform, unsaturated atmosphere quickly transfers its sensible heat to the surroundings as it cools to essentially the wet bulb temperature. Beyond this, droplets evaporate, but do so at roughly constant enthalpy, since the evaporation is exchanging sensible for latent heat. In the present LES, the ambient conditions seen by a droplet can change due both to two-way coupling with the spray and turbulent motions, and the droplet lifetimes are a function of size and turbulent transport.

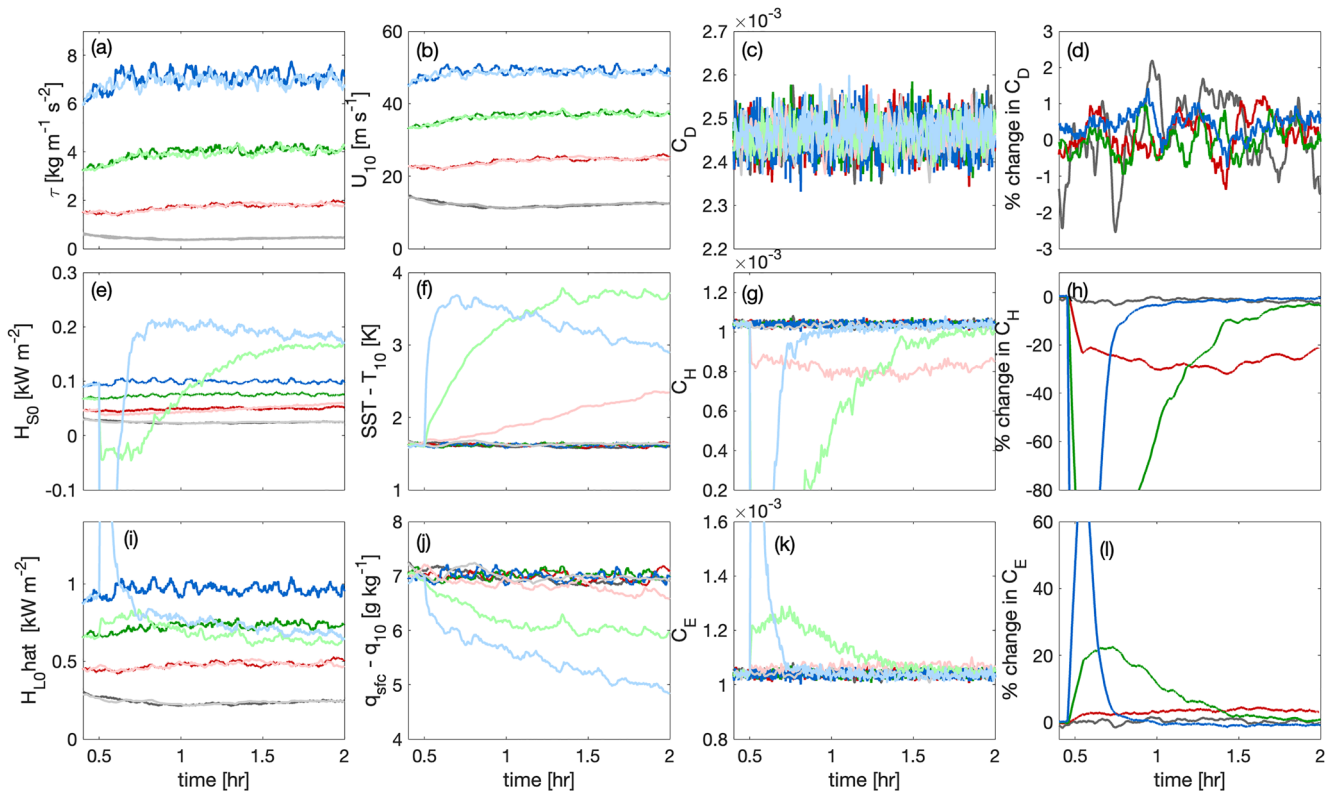


Figure 2. Top row: components of bulk C_D calculation (see Equation 4), τ (a), U_{10} (b), equivalent bulk C_D (c), and percentage change in C_D between the laden and unladen cases (d). Middle row: components of bulk C_H (see Equation 5), H_{S0} (e), $T_{sfc} - T_{10}$ (f), and equivalent bulk C_H (g), and percentage change in C_H between the laden and unladen cases (h). Bottom row: components of bulk C_E (see Equation 6), H_{L0} (i), $q_{sfc} - q_{10}$ (j), equivalent bulk C_E (k), and percentage change in C_E between the laden and unladen cases (l). For all plots the color representing each wind speed is as in Figure 1, and the darker color represents the unladen case while the lighter color represents the spray-laden case (e.g., case U60 is shown in dark green and case L60 in light green). On the right hand column the darker colors are used to represent the percentage change in the bulk transfer coefficients, and a 5-min moving average is applied to the data to reduce the impact of noise.

The introduction of spray starting at 30 min causes a temporary reduction in H_{S0} , even a reversal in sign for the highest wind speeds, followed by an increase above the unladen sensible heat flux. This adjustment process is most noticeable for cases L60 and L80, and at these speeds the increase in spray concentration accelerates the adjustment process. Likewise, at 30 min the spray causes an increase in H_{L0} above the unladen value, followed by a leveling-off below at times exceeding roughly 1 hr.

At the same time, and unlike the wind profile which was relatively unchanged between the laden and unladen cases, Figure 1 shows that the spray-laden cases are cooler and moister than their unladen counterparts, with larger impacts of spray seen as the wind speed (and thus spray concentration) increases. This is apparent in the time series of $SST - T_{10}$ and $q_{sfc} - q_{10}$ shown in Figures 2f and 2j, which are the primary components of the denominators of Equations 5 and 6 and indicate the substantial changes to the air-sea temperature and humidity differences due to the presence of spray. Spray causes the temperature difference to increase due to the decrease in 10-m temperature, while at the same time spray lowers the sea-air humidity difference by moistening the surface layer.

Noting that the flux coefficients depend on a combination of both the total fluxes H_{S0} and H_{L0} as well as the air-sea differences $SST - T_{10}$ and $q_{sfc} - q_{10}$ (each of which is influenced by the presence of spray) we plot the corresponding time series of C_H and C_E in Figures 2g and 2k. It is immediately clear that these quantities vary in time, and we divide each response into two regimes: an initial transient adjustment to the initiation of spray injection whose duration varies with wind speed, and a plateau period where C_H and C_E slowly level-off to a near-stationary value (nearly to saturation for the highest wind speeds).

The first regime is somewhat unphysical, in that the spun-up surface layer must rapidly adjust to the sudden injection of spray droplets—a situation that does not have an obvious environmental analog, except perhaps for

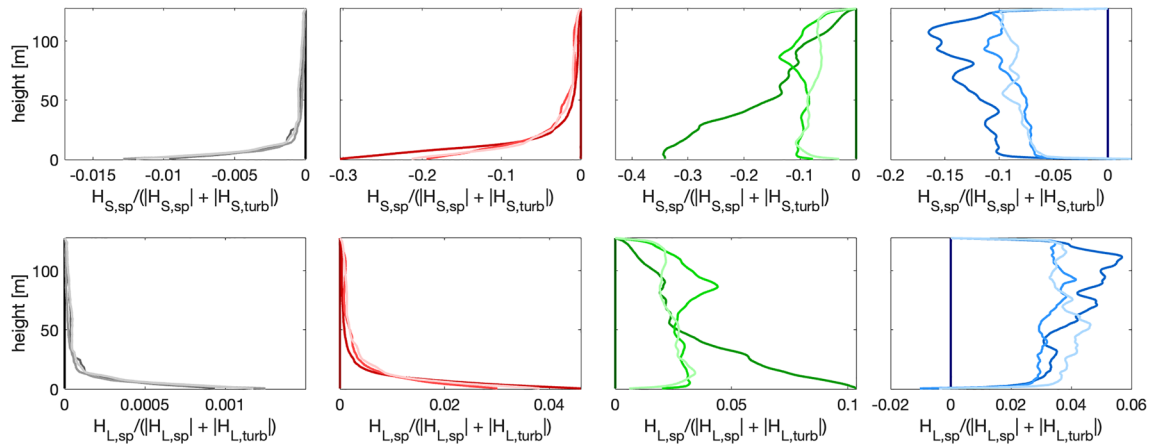


Figure 3. Top row: the fraction of the total sensible heat flux due to spray, $H_{S,sp}/(|H_{S,sp}| + |H_{S,turb}|)$. Bottom row: the fraction of the total latent heat flux due to spray, $H_{L,sp}/(|H_{L,sp}| + |H_{L,turb}|)$. Columns left to right represent cases L20, L40, L60, and L80 (same color scheme as in previous figures). In all panels lines show temporal progression through each simulation, with the darkest line at 30 min (just as spray injection begins), and increasingly lighter lines representing fluxes 60, 90, and 120 min.

a sudden enhancement in spray production due to, say, wind–wave alignment. During this time, at the highest wind speeds, the fluxes H_{S0} and H_{L0} experience a shock whose magnitude increases with wind speed but whose duration decreases. There is a corresponding sharp decrease in C_H and increase in C_E during this time, exceeding even an 80% change in the flux coefficients at the highest two wind speeds (Figures 2h and 2l). The negative values of C_H indicate a brief period where the total flux of sensible heat is downwards due to rapidly evaporating spray, despite a positive difference $SST - T_{10}$ —again, such a sudden jump in spray-mediated fluxes is highly unlikely in the environment.

In the second regime, however, the thermodynamic flux coefficients for the highest wind speeds (L60 and L80), after quickly adjusting to the injection of spray, actually approach their unladen values. Such a relaxation was also seen in the conceptually similar model framework of Onishi et al. (2016). It is only the L40 case which seems to maintain a C_H value which is substantially different than when spray is not present. In the high-wind cases, Figures 2e, 2f, 2i, and 2j show clearly that the recovery of C_H and C_E to their unladen values is not due to the absence of spray effects—indeed the total fluxes and the air-sea disequilibrium are greatly modified by the spray feedback. Instead, this recovery of C_H and C_E occurs as two things happen: the surface layer approaches full saturation (see Figure 1d), and when the changes to the fluxes H_{S0} and H_{L0} are offset by corresponding changes in the air-sea differences $SST - T_{10}$ and $q_{sfc} - q_{10}$. At these wind speeds, the feedback effects of spray are so strong that they rapidly result in a quasi-equilibrium where the approach to the unladen coefficients implies a turbulence-limited transport of spray-modified heat and moisture through the surface layer. For case L40, Figure 1d shows that the surface layer never reaches saturation due to the spray fluxes never being able to overcome the upwards transport of moisture; it is this case whose C_E and C_H maintain their (modest) difference with the unladen values.

To see this process more clearly, Figure 3 shows vertical profiles of the fraction of the total fluxes $H_S(z)$ and $H_L(z)$ carried by spray. For case L20 in the leftmost column, the spray production is sufficiently low that only a very small fraction of the total heat and moisture fluxes are due to spray. For case L40 (second column), we already see a negative, spray-mediated sensible heat flux that accounts for over 20% of the total flux near the surface and which rapidly decreases in magnitude with height. The spray-mediated fraction of the latent heat remains below 5%. Most notably, however, is that the shape of both profiles remains fairly robust in time, consistent with the stationarity of the flux coefficients see in Figure 2, and is related to the inability of spray to completely saturate the surface layer. Case L60 initially sees an even larger fraction of the total flux carried by the spray, but this decays over time, leveling off to a more vertically homogeneous profile which is around 10% for sensible and 3% for latent heat. Finally, case L80 has such a rapid adjustment that the total spray fraction, even at 60 min, has already decreased to a stationary value, where again spray only accounts for 10% of the sensible heat flux and less than 5% of the latent.

4. Discussion and Conclusions

Here we have used a combined LES and Lagrangian cloud model to investigate the impact of spray on the equivalent bulk transfer coefficients for momentum, heat and moisture in TC conditions. The model releases spray droplets based on 10-m wind speed following the Andreas (1998) SSGF, and we test four U_{10} values of 12, 24, 36, and 48 m s⁻¹. At each wind speed we run paired simulations: one unladen case and one where spray injection begins at 30 min and continues throughout the 2 hr simulation. We compare the unladen and laden simulations to examine how the spray affects the fluxes of heat, moisture, and momentum through the surface layer, including the impact on the bulk transfer coefficients C_D , C_H , and C_E . For all wind speeds, negligible spray effects were seen on momentum transfer or C_D .

What these simulations show for sensible and latent heat, however, is that only under certain circumstances can spray significantly modify the flux coefficients. Somewhat paradoxically, high-wind conditions that produce copious amounts of spray quickly saturate the surface layer and bring the reference temperature and humidity (i.e., T_{10} and q_{10}) back into balance with the fluxes. In these turbulence-limited conditions, the flux coefficients are nearly equal to their unladen value, since the spray can quickly replace any moisture that has been transported upwards. In the present simulations, it requires an unrealistic shock due to the abrupt initiation of spray injection to observe changes to C_H and C_E whose magnitude approach some of the more extreme values reported in the literature (Andreas et al., 2015; Komori et al., 2018), and even these are short-lived. As the spray moistens the layer—a process which occurs faster with more spray production—the flux coefficients relax back to their unladen, turbulence-dominated values. At the highest wind speeds, the fraction of the latent and sensible heat fluxes are 10% or less, and only exceed this when external processes (e.g., large scale horizontal advection) exist to efficiently remove moisture from the surface layer. This would suggest that the regions of a TC with the highest winds might not be the areas with the strongest spray influence—a phenomenon discussed recently by Barr et al. (2023). We note, however, that one of the underlying assumptions behind the LES framework employed here is that we are neglecting mean vertical advection in the domain (i.e., the domain is outside of the eyewall). If a mean updraft, or any other mechanism for that matter, could efficiently remove the moisture deposited by spray and prevent full saturation of the surface layer, then it is plausible that the flux coefficients could be more permanently modified.

We also suggest that the results here may help explain the continued discrepancies reported in the literature. Many spray models (Andreas et al., 2015; Bao et al., 2011; Mueller & Veron, 2014) predict a dramatic increase in the enthalpy flux coefficient C_K (usually assumed to be equal to C_H and C_E), but observational estimates often disagree. The only existing direct measurements from within a hurricane suggest that C_E and C_H do not have a strong wind speed dependence up to roughly 30 m s⁻¹ (Drennan et al., 2007). Despite high uncertainty, this seems to agree with other indirect estimates from within TCs out to much stronger wind speeds (Bell et al., 2012; Richter & Sullivan, 2014), and agrees with some laboratory experiments as well (Jeong et al., 2012). Other laboratory measurements, however, indicate a strong increase in the thermodynamic flux coefficients (Komori et al., 2018), yet in each of these the role of spray remains unclear. The current results emphasize the importance of the ambient environmental conditions (particularly the humidity), and models which fix the background temperature and humidity (Andreas, 2011) would likely overestimate the spray contribution to the fluxes. Laboratory studies likewise might inadvertently fix the ambient conditions by continuously bringing in relatively dry, surrounding air. Meanwhile the few observational estimates from within TCs, aside from being inherently uncertain, are averaged across multiple conditions in time or space and could therefore remove any localized enhancements due to spray.

Finally, the premise that the entire effect of spray can be observed from (or accounted for) in the flux coefficients, is faulty, and the results presented above highlight the need for spray models which account not only for the thermodynamic response of droplets, but also their proper coupling with the background temperature and humidity fields. While several past models neglect this two-way coupling, others do include it and see some similar qualitative trends to those reported above, although with some large quantitative differences owing to modeling assumptions. These include one of the original attempts at spray-turbulence coupling (Rouault et al., 1991), the bulk model of Bao et al. (2011), the Lagrangian stochastic model of Mueller and Veron (2014), the use of a cloud physics model to represent spray by Onishi et al. (2016), and the recent model of Barr et al. (2023). In each of these, the interfacial and spray-mediated fluxes of sensible and latent heat are solved simultaneously in a way that accounts for individual droplet microphysics and the response of the local environment, which we conclude is crucial for properly representing spray. Simply changing the flux coefficients C_H and/or C_E in a mesoscale model is insufficient.

We close by noting that the present simulations focus on a single SSGF and a single initial condition. As noted above, it is well-known that SSGFs at high winds are very uncertain, especially for the large droplets that contribute to spray-mediated fluxes (Ortiz-Suslow et al., 2016; Troitskaya et al., 2018). It is straightforward to alter the functional form of the SSGF in the present framework, although we do not anticipate any changes to our overall conclusions. The recent laboratory studies highlighting a stronger production of large droplets than previously considered would only act to accelerate the saturation process seen in the present LES simulations; that is, if more large droplets were included in the simulations, the relaxation of C_E and C_H would still occur, perhaps even more quickly, and our conclusion that spray cannot be captured simply by a modification to C_H or C_E would remain. The impact of neglecting other environmental processes not included here are less clear, including surface waves and storm-scale flow (i.e., not only considering a “patch” of the hurricane boundary layer). These remain the target of ongoing research.

Data Availability Statement

The dropsonde data used to generate the initial profile is available to be downloaded from the NOAA Hurricane Research Division website at https://www.aoml.noaa.gov/hrd/data_sub/dropsonde.html, or is available via the TC-DROPS database (Nguyen et al., 2019). The radius of maximum wind data used to filter the dropsonde profiles for use in the model initial profile are taken from the Tropical Cyclone Extended Best Track database, available online at https://rammb2.cira.colostate.edu/research/tropical-cyclones/tc_extended_best_track_dataset/. The NTLP large-eddy simulation and Lagrangian cloud model code is available at <https://github.com/RichterLab/NTLP/tree/SuperDroplet>. The data plotted in this manuscript, along with plotting scripts, are available at <https://doi.org/10.7274/sf268340371>.

References

- Andreas, E. L. (1998). A new sea spray generation function for wind speeds up to 32 m s⁻¹. *Journal of Physical Oceanography*, 28(11), 2175–2184. [https://doi.org/10.1175/1520-0485\(1998\)028<2175:ANSSGF>2.0.CO;2](https://doi.org/10.1175/1520-0485(1998)028<2175:ANSSGF>2.0.CO;2)
- Andreas, E. L. (2011). Fallacies of the enthalpy transfer coefficient over the ocean in high winds. *Journal of the Atmospheric Sciences*, 68(7), 1435–1445. <https://doi.org/10.1175/2011JAS3714.1>
- Andreas, E. L., & Emanuel, K. A. (2001). Effects of sea spray on tropical cyclone intensity. *Journal of the Atmospheric Sciences*, 58(24), 3741–3751. [https://doi.org/10.1175/1520-0469\(2001\)058<3741:EOSSOT>2.0.CO;2](https://doi.org/10.1175/1520-0469(2001)058<3741:EOSSOT>2.0.CO;2)
- Andreas, E. L., Mahrt, L., & Vickers, D. (2015). An improved bulk air-sea surface flux algorithm, including spray-mediated transfer. *Quarterly Journal of the Royal Meteorological Society*, 141(687), 642–654. <https://doi.org/10.1002/qj.2424>
- Bao, J.-W., Fairall, C. W., Michelson, S. A., & Bianco, L. (2011). Parameterizations of sea-spray impact on the air-sea momentum and heat fluxes. *Monthly Weather Review*, 139(12), 3781–3797. <https://doi.org/10.1175/MWR-D-11-00007.1>
- Barenblatt, G. I., Chorin, A. J., & Prostokishin, V. M. (2005). A note concerning the Lighthill “sandwich model” of tropical cyclones. *Proceedings of the National Academy of Sciences of the United States of America*, 102(32), 11148–11150. <https://doi.org/10.1073/pnas.0505209102>
- Barr, B., Chen, S. S., & Fairall, C. W. (2023). Seastate-dependent sea spray and air-sea heat fluxes in tropical cyclones: A new parameterization for fully coupled atmosphere-wave-ocean models. *Journal of the Atmospheric Sciences*. In Press. <https://doi.org/10.1175/JAS-D-22-0126.1>
- Bell, M. M., Montgomery, M. T., & Emanuel, K. A. (2012). Air-sea enthalpy and momentum exchange at major hurricane wind speeds observed during CBLAST. *Journal of the Atmospheric Sciences*, 69(11), 3197–3222. <https://doi.org/10.1175/JAS-D-11-0276.1>
- Bryan, G. H., Worsnop, R. P., Lundquist, J. K., & Zhang, J. A. (2017). A simple method for simulating wind profiles in the boundary layer of tropical cyclones. *Boundary-Layer Meteorology*, 162(3), 475–502. <https://doi.org/10.1007/s10546-016-0207-0>
- Chen, X., Bryan, G. H., Zhang, J. A., Cione, J. J., & Marks, F. D. (2021). A framework for simulating the tropical cyclone boundary layer using large-eddy simulation and its use in evaluating PBL parameterizations. *Journal of the Atmospheric Sciences*, 78, 3559–3574. <https://doi.org/10.1175/JAS-D-20-0227.1>
- Deardorff, J. W. (1980). Stratocumulus-capped mixed layers derived from a three-dimensional model. *Boundary-Layer Meteorology*, 18(4), 495–527. <https://doi.org/10.1007/bf00119502>
- Demuth, J. L., DeMaria, M., & Knaff, J. A. (2006). Improvement of advanced microwave sounding unit tropical cyclone intensity and size estimation algorithms. *Journal of Applied Meteorology and Climatology*, 45(11), 1573–1581. <https://doi.org/10.1175/JAM2429.1>
- Drennan, W. M., Zhang, J. A., French, J. R., McCormick, C., & Black, P. G. (2007). Turbulent fluxes in the hurricane boundary layer. Part II: Latent heat flux. *Journal of the Atmospheric Sciences*, 64(4), 1103–1115. <https://doi.org/10.1175/JAS3889.1>
- Emanuel, K. A. (1995). Sensitivity of tropical cyclones to surface exchange coefficients and a revised steady-state model incorporating eye dynamics. *Journal of the Atmospheric Sciences*, 52(22), 3969–3976. [https://doi.org/10.1175/1520-0469\(1995\)052<3969:sotets>2.0.co;2](https://doi.org/10.1175/1520-0469(1995)052<3969:sotets>2.0.co;2)
- Fairall, C. W., Banner, M. L., Peirson, W. L., Asher, W., & Morison, R. P. (2009). Investigation of the physical scaling of sea spray spume droplet production. *Journal of Geophysical Research*, 114(C10), C10001. <https://doi.org/10.1029/2008JC004918>
- Fairall, C. W., Kepert, J. D., & Holland, G. J. (1994). The effect of sea spray on surface energy transports over the ocean. *The Global Atmosphere and Ocean System*, 2, 121–142.
- Jeong, D., Haus, B. K., & Donelan, M. A. (2012). Enthalpy transfer across the air-water interface in high winds including spray. *Journal of the Atmospheric Sciences*, 69(9), 2733–2748. <https://doi.org/10.1175/JAS-D-11-0260.1>
- Komori, S., Iwano, K., Takagaki, N., Onishi, R., Kurose, R., Takahashi, K., & Suzuki, N. (2018). Laboratory measurements of heat transfer and drag coefficients at extremely high wind speeds. *Journal of Physical Oceanography*, 48(4), 959–974. <https://doi.org/10.1175/JPO-D-17-0243.1>
- Lewis, E. R., & Schwartz, S. E. (2004). *Sea salt aerosol production: Mechanisms, methods, measurements, and models—A critical review*. American Geophysical Union.

Acknowledgments

This research was funded by the Office of Naval Research Directed Research Initiative N00014-20-1-2060 entitled Tropical Cyclone Rapid Intensification (TCRI). Computer resources were made available through the Notre Dame Center for Research Computing and the DoD High Performance Computing Modernization Program.

- MacMillan, T., Shaw, R. A., Cantrell, W. H., & Richter, D. H. (2022). Direct numerical simulation of turbulence and microphysics in the Pi Chamber. *Physical Review Fluids*, 7(2), 020501. <https://doi.org/10.1103/PhysRevFluids.7.020501>
- Mallen, K. J., Montgomery, M. T., & Wang, B. (2005). Reexamining the near-core radial structure of the tropical cyclone primary circulation: Implications for vortex resiliency. *Journal of the Atmospheric Sciences*, 62(2), 408–425. <https://doi.org/10.1175/JAS-3377.1>
- Moeng, C.-H. (1984). A large-eddy-simulation model for the study of planetary boundary-layer turbulence. *Journal of the Atmospheric Sciences*, 41(13), 2052–2062. [https://doi.org/10.1175/1520-0469\(1984\)041<2052:ALESMF>2.0.CO;2](https://doi.org/10.1175/1520-0469(1984)041<2052:ALESMF>2.0.CO;2)
- Mueller, J. A., & Veron, F. (2014). Impact of sea spray on air-sea fluxes. Part II: Feedback effects. *Journal of Physical Oceanography*, 44(11), 2835–2853. <https://doi.org/10.1175/JPO-D-13-0246.1>
- Nguyen, L. T., Rogers, R., Zawislak, J., & Zhang, J. A. (2019). Assessing the influence of convective downdrafts and surface enthalpy fluxes on tropical cyclone intensity change in moderate vertical wind shear. *Monthly Weather Review*, 147(10), 3519–3534. <https://doi.org/10.1175/MWR-D-18-0461.1>
- Onishi, R., Fuchigami, H., Matsuda, K., & Takahashi, K. (2016). Detailed cloud microphysics simulation for investigation into the impact of sea spray on air-sea heat flux. *Flow, Turbulence and Combustion*, 97(4), 1111–1125. <https://doi.org/10.1007/s10494-016-9766-x>
- Ortiz-Suslow, D. G., Haus, B. K., Mehta, S., & Laxague, N. J. M. (2016). Sea spray generation in very high winds. *Journal of the Atmospheric Sciences*, 73(10), 3975–3995. <https://doi.org/10.1175/JAS-D-15-0249.1>
- Peng, T., & Richter, D. (2020). Influences of Polydisperse Sea spray size distributions on model predictions of air-sea heat fluxes. *Journal of Geophysical Research: Atmospheres*, 125(14), e2019JD032326. <https://doi.org/10.1029/2019jd032326>
- Peng, T., & Richter, D. H. (2017). Influence of evaporating droplets in the turbulent marine atmospheric boundary layer. *Boundary-Layer Meteorology*, 165(3), 1–22. <https://doi.org/10.1007/s10546-017-0285-7>
- Peng, T., & Richter, D. H. (2019). Sea spray and its feedback effects: Assessing bulk algorithms of air-sea heat fluxes via direct numerical simulations. *Journal of Physical Oceanography*, 49(6), 1403–1421. <https://doi.org/10.1175/JPO-D-18-0193.1>
- Rastigejev, Y., & Suslov, S. A. (2019). Effect of evaporating sea spray on heat fluxes in a marine atmospheric boundary layer. *Journal of Physical Oceanography*, 49(7), 1927–1948. <https://doi.org/10.1175/JPO-D-18-0240.1>
- Richter, D. H., Bohac, R., & Stern, D. P. (2016). An assessment of the flux profile method for determining air-sea momentum and enthalpy fluxes from dropsonde data in tropical cyclones. *Journal of the Atmospheric Sciences*, 73(7), 2665–2682. <https://doi.org/10.1175/JAS-D-15-0331.1>
- Richter, D. H., MacMillan, T., & Wainwright, C. (2021). A Lagrangian cloud model for the study of marine fog. *Boundary-Layer Meteorology*, 282(2–3), 523–542. <https://doi.org/10.1007/s10546-020-00595-w>
- Richter, D. H., & Sullivan, P. P. (2014). The sea spray contribution to sensible heat flux. *Journal of the Atmospheric Sciences*, 71(2), 640–654. <https://doi.org/10.1175/JAS-D-13-0204.1>
- Rogers, R., Aberson, S., Black, M., Black, P., Cione, J., Dodge, P., et al. (2006). The intensity forecasting experiment: A NOAA multiyear field program for improving tropical cyclone intensity forecasts. *Bulletin of the American Meteorological Society*, 87(11), 1523–1537. <https://doi.org/10.1175/BAMS-87-11-1523>
- Rouault, M. P., Mestayer, P. G., & Schiestel, R. (1991). A model of evaporating spray droplet dispersion. *Journal of Geophysical Research*, 96(C4), 7181–7200. <https://doi.org/10.1029/90JC02569>
- Shima, S., Kusano, K., Kawano, A., Sugiyama, T., & Kawahara, S. (2009). The super-droplet method for the numerical simulation of clouds and precipitation: A particle-based and probabilistic microphysics model coupled with a non-hydrostatic model. *Quarterly Journal of the Royal Meteorological Society*, 135(642), 1307–1320. <https://doi.org/10.1002/qj.441>
- Smith, M. H., Park, P. M., & Consterdine, I. E. (1993). Marine aerosol concentrations and estimated fluxes over the sea. *Quarterly Journal of the Royal Meteorological Society*, 119(512), 809–824. <https://doi.org/10.1002/qj.49711951211>
- Sroka, S., & Emanuel, K. (2021). A review of parameterizations for enthalpy and momentum fluxes from sea spray in tropical cyclones. *Journal of Physical Oceanography*, 51, 3053–3069. <https://doi.org/10.1175/jpo-d-21-0023.1>
- Sullivan, P. P., McWilliams, J. C., & Moeng, C.-H. (1994). A subgrid-scale model for large-eddy simulation of planetary boundary-layer flows. *Boundary-Layer Meteorology*, 71(3), 247–276. <https://doi.org/10.1007/BF00713741>
- Troitskaya, Y. I., Kandaurov, A., Ermakova, O., Kozlov, D., Sergeev, D., & Zilitinkevich, S. (2018). The “Bag Breakup” spume droplet generation mechanism at high winds. Part I: Spray generation function. *Journal of Physical Oceanography*, 48(9), 2167–2188. <https://doi.org/10.1175/jpo-d-17-0104.1>
- Veron, F. (2015). Ocean spray. *Annual Review of Fluid Mechanics*, 47(1), 507–538. <https://doi.org/10.1146/annurev-fluid-010814-014651>